

Wavelength tracking with thermally controlled silicon resonators

Ciyuan Qiu, Jie Shu, Zheng Li Xuezhi Zhang, and Qianfan Xu*

Department of Electrical and Computer Engineering, Rice University, Houston, Texas 77005, USA

**qianfan@rice.edu*

Abstract: We experimentally demonstrate feedback controlling of the resonant wavelength of a silicon dual-ring resonator. The feedback signal is the difference in optical scattering from the two coupled microring resonators, and the control mechanism is based on thermo-optic tuning with micro-heaters. This control scheme keeps the central wavelength of the resonator aligning with the input wavelength, which can be used to compensate fabrication variations, environmental temperature shift and the drift of laser wavelength. This feedback control scheme allows microring-based electro-optic modulators to be used in a dynamic environment.

©2011 Optical Society of America

OCIS codes: (130.0130) Integrated optics; (230.5750) Resonators.

References and links

1. Q. Xu, S. Manipatruni, B. Schmidt, J. Shakya, and M. Lipson, "12.5 Gbit/s carrier-injection-based silicon microring silicon modulators," *Opt. Express* **15**(2), 430–436 (2007).
2. P. Dong, S. Liao, D. Feng, H. Liang, D. Zheng, R. Shafiqi, C.-C. Kung, W. Qian, G. Li, X. Zheng, A. V. Krishnamoorthy, and M. Asghari, "Low Vpp, ultralow-energy, compact, high-speed silicon electro-optic modulator," *Opt. Express* **17**(25), 22484–22490 (2009).
3. M. R. Watts, D. C. Trotter, R. W. Young, and A. L. Lentine, "Ultralow power silicon microdisk modulators and switches," in *Proceedings of 5th IEEE International Conference on Group IV Photonics (IEEE 2008)*, pp. 4–6.
4. Q. Xu, D. Fattal, and R. G. Beausoleil, "Silicon microring resonators with 1.5-microm radius," *Opt. Express* **16**(6), 4309–4315 (2008).
5. A. V. Krishnamoorthy, R. Ho, X. Zheng, H. Schwetman, J. Lexau, P. Koka, G. Li, I. Shubin, and J. E. Cunningham, "Computer systems based on silicon photonic interconnects," *Proc. IEEE* **97**(7), 1337–1361 (2009).
6. J. Teng, P. Dumon, W. Bogaerts, H. Zhang, X. Jian, X. Han, M. Zhao, G. Morthier, and R. Baets, "Athermal Silicon-on-insulator ring resonators by overlaying a polymer cladding on narrowed waveguides," *Opt. Express* **17**(17), 14627–14633 (2009).
7. P. Alipour, A. H. Atabaki, A. A. Eftekhar, and A. Adibi, "Titania-Clad Microresonators on SOI With Athermal Performance," In *Conference on Lasers and Electro-Optics / Quantum Electronics and Laser Science Conference (CLEO/QELS 2010)*, paper JThE44.
8. B. Guha, B. B. C. Kyotoku, and M. Lipson, "CMOS-compatible athermal silicon microring resonators," *Opt. Express* **18**(4), 3487–3493 (2010).
9. Q. Xu, "Silicon dual-ring modulator," *Opt. Express* **17**(23), 20783–20793 (2009).
10. H.-Y. Ng, M. R. Wang, D. Li, X. Wang, J. Martinez, R. R. Panepucci, and K. Pathak, "4 x 4 wavelength reconfigurable photonic switch based on thermally tuned silicon microring resonators," *Opt. Eng.* **47**, 044601–044608 (2008).
11. L. Chen, N. Sherwood-Droz, and M. Lipson, "Compact bandwidth-tunable microring resonators," *Opt. Lett.* **32**(22), 3361–3363 (2007).
12. Y. A. Vlasov, M. O'Boyle, H. F. Hamann, and S. J. McNab, "Active control of slow light on a chip with photonic crystal waveguides," *Nature* **438**(7064), 65–69 (2005).
13. J. M. Elson, "Diffraction and diffuse scattering from dielectric multilayers," *J. Opt. Soc. Am. A* **69**, 682–694 (1976).
14. J. A. Sánchez-Gil and M. Nieto-Vesperinas, "Light scattering from random rough dielectric surfaces," *J. Opt. Soc. Am. A* **8**(8), 1270–1286 (1991).
15. M. Nieto-Vesperinas and J. M. Soto-Crespo, "Monte Carlo simulations for scattering of electromagnetic waves from perfectly conductive random rough surfaces," *Opt. Lett.* **12**(12), 979–981 (1987).
16. L. Chen, P. Dong, and M. Lipson, "High performance germanium photodetectors integrated on submicron silicon waveguides by low temperature wafer bonding," *Opt. Express* **16**(15), 11513–11518 (2008).

17. Q. Xu, S. Sandhu, M. L. Povinelli, J. Shakya, S. Fan, and M. Lipson, "Experimental realization of an on-chip all-optical analogue to electromagnetically induced transparency," *Phys. Rev. Lett.* **96**(12), 123901 (2006).
 18. Q. Xu, P. Dong, and M. Lipson, "Breaking the Delay-Bandwidth Limit in a Photonic Structure," *Nat. Phys.* **3**(6), 406–410 (2007).
-

1. Introduction

Silicon microring and microdisk modulators [1–3] are key enablers for dense wavelength-division multiplexing (DWDM) interconnection systems [4] due to their high modulation speed and low power consumption. The wavelength sensitivity of the modulators, while important for its use in a DWDM system, makes them difficult to be used in a dynamic system with variations in the environmental temperature and the drift of the wavelength of the optical source. Besides that, current fabrication technologies cannot guarantee the as-fabricated modulators across a whole wafer to work precisely at their designed wavelengths [5]. Various approaches have been demonstrated to make temperature insensitive microring resonators, including using resonator claddings with negative thermo-optic coefficient [6,7] and tailoring the degree of optical confinement in silicon waveguides [8]. However, these approaches do not compensate variations in the fabrication process or the drift of the laser wavelength.

We have proposed an optical modulator based on two coupled microring resonators [9], which have higher optical bandwidth and lower power consumption than the single-ring modulators. While the higher optical bandwidth makes it less sensitive to temperature or wavelength variations, the tolerance range is still limited. To compensate simultaneously for all the mechanisms that cause wavelength misalignment, including the environmental temperature variation, laser wavelength drift and fabrication imperfections, thermo-optics tuning [10–12] with an active feedback control is likely to be required for each modulator.

The next question is how to conveniently obtain a feedback signal that precisely indicates the detuning between the laser wavelength and the modulator operation wavelength, even when the modulator is actively working. The dual-ring modulator we proposed in [9] provides such a feedback signal, which is based on the difference in optical intensities in the two rings. When the input light is at the central wavelength between the resonances of the two individual rings, which is the optimal operation wavelength of a dual-ring modulator, the optical intensity in the two rings are equal. When the optical intensities in the two rings differ, by measuring the sign of the difference, we know which ring resonance is closer to the wavelength of light, and thus which way to tune the two rings to bring the laser wavelength back to the center.

The optical intensity inside each ring can be measured externally from its scattered optical power [13–15]. In this paper, we experimentally demonstrate an active feedback control system where the feedback signal is the difference in optical scattering from the two microring resonators, and the control mechanism is based on thermo-optic tuning with micro-heaters. We show that the control system can keep the central wavelength of the coupled resonator aligning with the laser wavelength when we intentionally shift the laser wavelength. Since optical scattering is used as the feedback signal, this method is nonintrusive to the device operation.

2. Device structure, fabrication and test setup

The structure of the dual-ring resonator is shown in Fig. 1(a). The two microrings with slightly different radii around 2.5 μm are side coupled to two parallel waveguides. The center-to-center distance between the two ring resonators is 7.85 μm . The width of the ring is about 460 nm. Each ring has a C-shaped micro-heater on top of a 1- μm -thick SiO_2 waveguide cladding. The device was fabricated on a silicon-on-insulator platform with 3- μm buried oxide using a scanning electron microscope (SEM)-based e-beam lithography system. The pattern is first defined on a layer of negative e-beam resist by an externally controlled SEM with an accelerating voltage of 30 kV. The pattern is then transferred to the silicon layer with a Cl_2 -

based reactive ion etching process. After deposition of a 1 μm -thick SiO_2 cladding by plasma enhanced chemical-vapor deposition, a 150-nm-thick chromium heater and a 30-nm-thick gold pad are made by e-beam lithography and lift-off process.

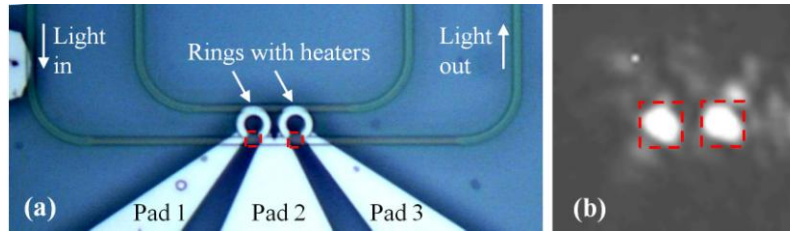


Fig. 1. (a) Top-view microscopic picture of the dual-ring resonator with micro-heaters. The two red dash squares make the two scattering collected regions. (b) Infrared scattering image of the device with optical input at the central wavelength. Scattered optical powers are obtained by calculate the average brightness inside the two dashed squares.

Figure 2 shows the experimental setup for measuring the transmission spectrum in the feedback control process. The polarization of the tunable laser is adjusted by a polarization controller and a polarizer to be quasi-TE. Then the light is focused by a lens onto one end of a U-shaped waveguide [4]. The output light at the other end of the U-shaped waveguide is collimated by the same lens and is sent to a detector.

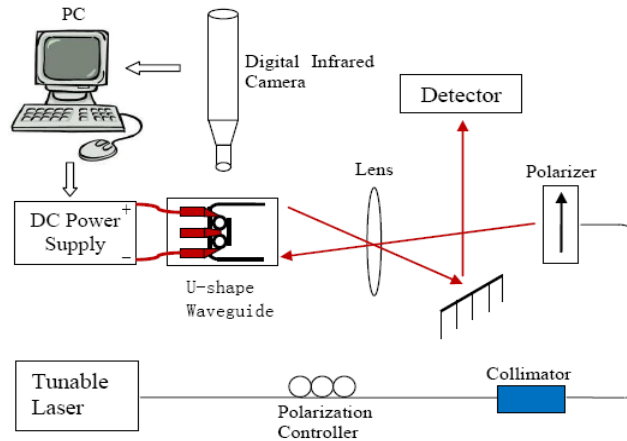


Fig. 2. Schematic of the experimental setup for measuring the transmission spectrum of the resonators and to measure the optical scattering for the feedback control process.

While the scattered power from the two rings can be measured with Ge-based photodetectors integrated on top of the resonators [16], for proof-of-principle purpose, we measure here the scattered power from a digital infrared camera that takes the top view image of the device. Figure 1(b) shows a top-view picture of the light scattered from the two microrings when the device is working at the central wavelength. The scattered optical powers from the two rings are obtained by calculating the average brightness inside the two dashed squares. One can see from the figure that, as we expected, the scattered powers from the two rings are very close at this condition. The scattering measurements from the camera were sent to a Labview-based program which is used to control the voltage that need to be applied on the micro-heaters for the feedback control.

3. Optical properties of the device

We measured the transmission spectrum of the couple resonator, which is shown as the dots in Fig. 3(a). A sharp transmission peak around λ_0 can be seen on the spectrum. This peak comes

from a supermode which is the result of coherent coupling between the two rings through the two parallel waveguides [17]. The full-width at half-maximum (FWHM) bandwidth of the supermode is 0.8 nm. The two minimal transmission points on the spectrum (λ_1 and λ_2) correspond to the resonant wavelengths of the two individual rings. As the red line in Fig. 3(a) shows, the measured transmission can be fitted well with a theoretical model [18]. From the fitting, we found the optical parameters of the fabricated device to be: the detuning between the two ring resonances is $\lambda_2 - \lambda_1 = 2.42$ nm; intrinsic Q's of these two rings are both $\sim 10,000$; and the power coupling efficiency between each ring and its adjacent waveguide is about 28%.

We measured the optical scattering from the two rings at different wavelengths, which is shown as the black and red dots in Fig. 3(b). The measured scattering spectrum agrees well with the theoretical spectra of optical intensity inside the rings, calculated with the same model and the same parameters obtained by fitting the transmission spectrum. The calculated optical intensities inside the two rings are shown as the black and red lines in Fig. 3(b). Without the supermode, the intensity inside each ring would peak at its own resonant wavelength. Due to the presence of the supermode, the intensity in each is enhanced, and the enhancement peaks at the supermode wavelength λ_0 . Therefore, the scattering from each ring reaches its maximum at a wavelength between its own resonant wavelength and λ_0 .

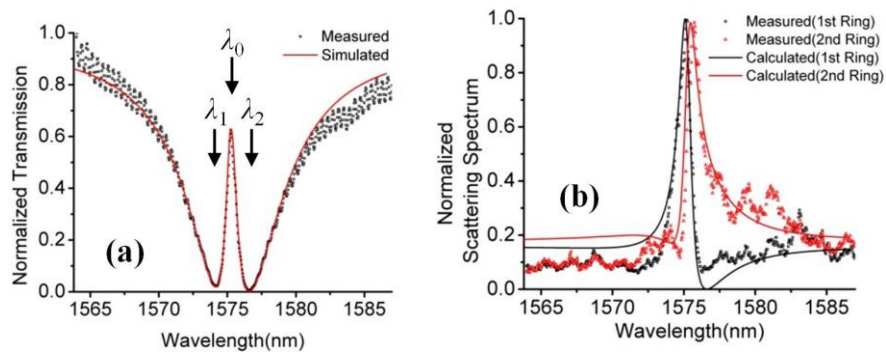


Fig. 3. Transmission and scattering spectra of the dual-ring resonator. (a) The measured (black dots) and fitted transmission spectra (the red line) [17]. λ_0 is the central wavelength of the supermode. λ_1 and λ_2 are the resonance wavelengths of the two individual rings. (b) The normalized scattering spectra for the two rings (red and black dots) and the spectra calculated using the parameters obtained from the fitting shown in (a) (red and black lines).

4. Thermo-optic tuning

In Fig. 4(a), we show the measured spectrum of the difference in optical scattering from the two rings and the measured transmission spectrum. One can see from the figure that the wavelength where the scattering difference crosses zero (λ_S) is close to the central wavelength of the supermode (λ_0). While λ_0 is the optimal operation wavelength, λ_S will be the target wavelength for the feedback control scheme that we will show later. The misalignment $\lambda_S - \lambda_0$ is 0.07 nm, which is less than 10% of the FWHM of the supermode. As the result, the transmission at λ_S is 95% of the peak transmission at λ_0 . As the wavelength moving away from the resonances, the scattering difference also approaches zero. There is thus a finite wavelength range for the feedback control scheme to work, which depends on the signal-to-noise ratio and the background scattering. For this device, the laser wavelength has to initial fall within $\sim \pm 1.5$ nm around λ_0 in order for the feedback control system to automatically tune λ_0 to the laser wavelength.

When the dual-ring modulator is operating, the wavelength detuning between the two rings varies, resulting in appearing (the ON state) or disappearing (the OFF state) of the central transmission peak [9]. In order to show that we can use the average scattering

difference as the feedback signal when the modulator is operating, we need to show that λ_S is closely aligned with λ_0 at both the ON state and the OFF state, and any transitional state in between of them. To do that, we change the detuning between the two ring resonances by applying electrical current on one of the micro-heaters, and measure how the ratio P_S/P_0 , where P_S and P_0 are the optical output power at λ_S and λ_0 , varies. As shown in Fig. 4(b), the ratio P_S/P_0 remains larger than 92% for different resonance wavelength detuning between the two rings. This indicates that misalignment $\lambda_S - \lambda_0$ is always small, and we can reliably use the difference between the average scattered powers of the two rings as the feedback signal even when the wavelength detuning between the two rings is actively changing for the purpose of modulation.

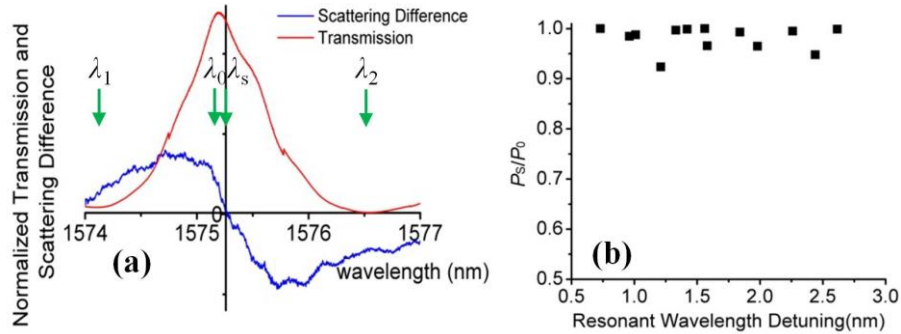


Fig. 4. (a) Measured transmission spectrum (the red line) and scattering difference (the blue line) near the central wavelength (λ_0). λ_S is the wavelength where the scattering difference crosses zero (b) Power efficiency at different resonance wavelength detuning $\lambda_2 - \lambda_1$. P_S is the optical output power at λ_S and P_0 is the optical output power at λ_0 .

Two micro-heaters made of chromium thin-film resistors are used to control the temperature of the two microring resonators, which red shift the ring resonances at a rate of ~ 0.1 nm/ $^{\circ}$ C. In the control process, the same current was injected into both micro-heaters simultaneously. During this process, the shape of the dual-ring resonance is kept unchanged while the central wavelength λ_0 is red shifted. Figure 5(a) shows the transmission spectrum at different heating powers. The resonance red-shifts as the heating power increases and the temperature of the devices rises as we expected. The peak transmission at central wavelength has a little variation, which is due to a weak Fabry-Perot (FP) interference from the reflection at the input and output ends of the waveguide. In Fig. 5(b), we plotted the relationship between the central wavelength (λ_0) shift and the heating power, from which we calculated a

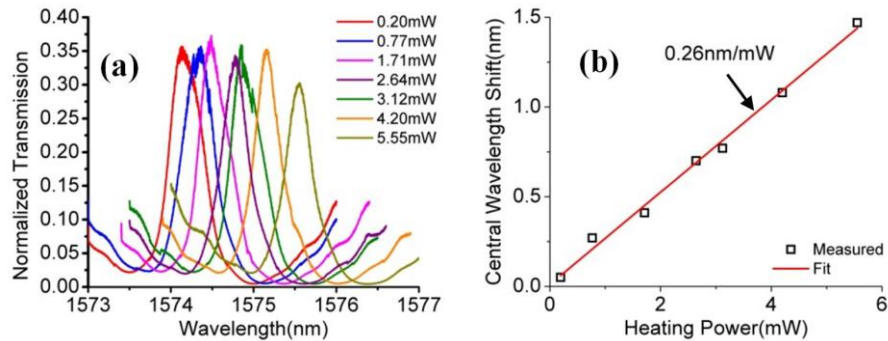


Fig. 5. (a) Normalized transmission spectra with different heating powers on the integrated micro-heaters (b) The shift of central wavelength at different heating powers.

power efficiency of the thermo-optic tuning to be 0.26 nm/mW. We measured that the detuning between λ_s (the wavelength where the scattering from the two rings equal) and λ_0 is always smaller than 0.09 nm (11% of FWHM) over the entire tuning range. This ensures that we can successfully track the central wavelength using the scattering difference as the feedback signal.

5. Wavelength tracking with feedback control

We built a feedback control system with a Labview-based program that continuously measures the difference in scattering from the two rings, and adjusts the current injected on the two heaters according to the sign of the difference. To demonstrate the tracking capability, we sweep the wavelength of the input laser from 1574.4nm to 1574.7nm in 150 seconds after the system is locked at the initial laser wavelength of 1574.4nm. If the feed-back control system is turned off during the wavelength sweep, the transmission would drop over time as that shown by the green line in Fig. 6(a). When the feed-back control system is kept on, the central wavelength of the coupled resonator successfully tracks the wavelength sweep and the output power remains high, which is shown as the blue line in Fig. 6(a). The blue line shows small variations (~10%) due to a weak Fabry-Perot (FP) interference. The red curve shows the total electrical power consumption for the heater. The corresponding scattering light from two selected regions in the feedback control process is shown in Fig. 6(b). The scattering from the first ring always equals to that from the second ring within the noise limit. However, the intensity has a variation which is also due to the F-P mode interference.

The micro-heater can only heat up the device and red shift its resonances. In order to track both a red-shift and a blue-shift of the laser wavelength, the resonator should be designed to work at an elevated temperature above that of the substrate, so that both blue-shift and red-shift of the resonances can be obtained by either increasing or decreasing the heating power. Note that we did not observe any performance degradation of the resonator during the heating processes in our experiment.

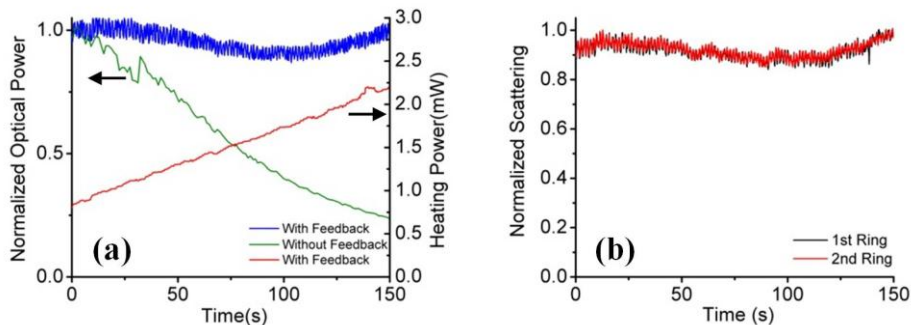


Fig. 6. The active feedback control process. (a) Normalized optical transmission with (the blue line) and without (the green line) the feedback control process. The red line shows the power applied on the heater. (b) The normalized scattering signal for the two rings during the control process.

6. Conclusion

We demonstrate feedback controlling of the resonant wavelength of a silicon dual-ring resonator. The feedback signal is the difference in optical scattering from the two coupled microring resonators, and the controlling mechanism is based on thermo-optic tuning with micro-heaters. We demonstrated that the operational wavelength of the dual ring resonator can track the wavelength of the input laser while the laser wavelength is swept.